Clays and Clay Minerals, Vol. 34, No. 5, 572–580, 1986.

SUPERGENE VERMICULITIZATION OF A MAGNESIAN CHLORITE: IRON AND MAGNESIUM REMOVAL PROCESSES

DOMINIQUE PROUST,[1] JEAN-PAUL EYMERY,[2] AND DANIEL BEAUFORT[3]

[1] Laboratoire de Pétrologie de la Surface, Université de Poitiers
86022 Poitiers Cédex, France

[2] Laboratoire de Métallurgie Physique, Université de Poitiers
86022 Poitiers Cédex, France

[3] Laboratoire de Pétrologie des Altérations Hydrothermales, Université de Poitiers
86022 Poitiers Cédex, France

Abstract—An X-ray powder diffraction study of a vermiculitized chlorite in an amphibole schist near Limoges, France, shows the following weathering sequence: chlorite → ordered interstratified chlorite/vermiculite → vermiculite. Mössbauer spectroscopy indicates that vermiculitization proceeded by the release of ferrous iron from the 2:1 mica layer of the chlorite. The ferric iron content of the vermiculite product is almost the same as that of the initial chlorite. Infrared spectroscopy and chemical microprobe analyses show that Mg was preferentially extracted from the hydroxide sheet of the chlorite, whereas the Si and Al contents progressively increased to the point of the formation of a pure dioctahedral aluminous vermiculite. The Si, Al, and Mg removal processes support currently accepted vermiculitization mechanisms, but the behavior of Fe is slightly different. In this weathering sequence, vermiculitization does not appear to have taken place by the oxidation of Fe^{2+}, but rather, by the simultaneous leaching of Fe^{2+} and Mg.

Key Words—Chlorite, Infrared spectroscopy, Interstratified chlorite/vermiculite, Iron, Mössbauer spectroscopy, Vermiculite, Weathering.

Résumé—L'analyse par diffraction de rayons X d'une chlorite magnésienne, dans une arène d'amphibolite, caractérise la séquence d'altération suivante: chlorite → interstratifié régulier chlorite/vermiculite → vermiculite. La spectroscopie Mössbauer indique que la vermiculitisation opère par libération du fer, à l'état ferreux, hors du feuillet 2:1 de la chlorite. La teneur en fer ferrique de la vermiculite est voisine de celle de la chlorite. Les analyses à la microsonde et en spectroscopie infrarouge montrent que Mg est préférentiellement libéré de la couche brucitique de la chlorite tandis que les teneurs en Si et Al augmentent avec l'altération jusqu'à la cristallisation d'une vermiculite dioctaédrique alumineuse. Les méchanismes de libération de Si, Al, et Mg sont semblables à ceux habituellement admis pour la vermiculitisation, mais le comportement du fer est différent. Dans cette séquence d'altération, la vermiculitisation ne procède pas par oxydation du fer, mais par départ simultané du fer ferreux et du magnésium.

INTRODUCTION

Supergene vermiculitization of chlorites through intermediate stages of interstratified chlorite/vermiculite is one of the most common weathering sequences reported in the literature (Johnson, 1964; Gilkes and Little, 1972; Herbillon and Makumbi, 1975; Adams, 1976; Bain, 1977; Rabenhorst *et al.*, 1982; Ross *et al.*, 1982). Experimental data from numerous investigators (e.g., Ross, 1975; Ross and Kodama, 1974, 1976; Senkayi *et al.*, 1981) have demonstrated that vermiculitization of chlorite can be readily achieved by a thermal treatment of the chlorite above its dehydroxylation temperature (610°C) followed by an acid dissolution of its hydroxide sheet. These authors (as well as Makumbi and Herbillon, 1972) concluded from infrared, differential thermal, and more recently, Mössbauer analyses (Goodman and Bain, 1979; Borggaard *et al.*, 1982), that the experimental vermiculitization was initiated by the oxidation of ferrous iron through a reaction scheme of the form: $[Fe^{2+}OH]^+ \rightarrow [Fe^{3+}O]^+ + H^+ + e^-$ in the structural unit, followed by the loss of ferric iron and magnesium from the hydroxide sheet.

The present investigation was designed to determine whether or not this experimental process could indeed explain the supergene vermiculitization of a magnesian, low-iron, chlorite in a weathering profile which formed under temperate conditions from an amphibole schist.

MATERIALS AND METHODS

Materials

Chlorite was collected from a weathered amphibole schist south of Limoges, France (Figure 1). The unweathered rock at the bottom of the outcrop was a foliated amphibolite made up of quartz (17%), green hornblende (42%), andesine (33%), and chlorite (8%); its weathering profile consisted of three levels of alteration, from bottom to top: (1) a saprock, above the unweathered rock, in which the coherent foliated struc-

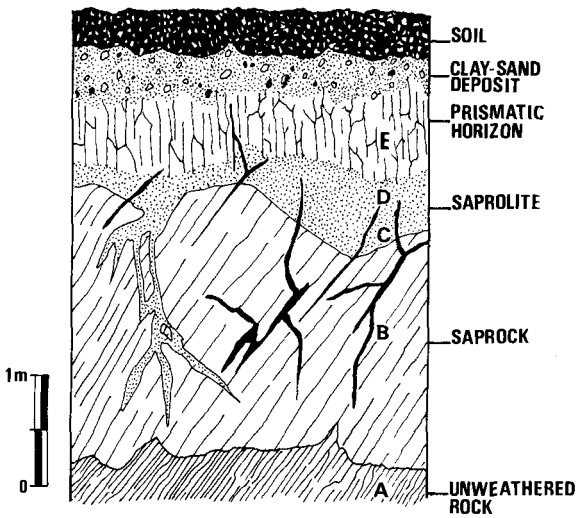

Figure 1. Sketch of the amphibolite weathering profile; letters refer to sampling locations.

ture was still preserved and in which primary minerals were contiguous; (2) a saprolite in which the texture of the original rock was destroyed and replaced by a clayey weathering matrix surrounding relicts of primary minerals; and (3) a new, prismatic,[4] horizon generated by the wetting and drying movements of the deeply argillized rock. The weathering profile was covered by an allochthonous clay-sand deposit containing quartz, iron pisolites, and primary quartz and hornblende inherited from the parent rock.

Chlorite (125–200 μm) was extracted from the unweathered rock (sample A in Figure 1), the saprock (sample B), and the saprolite (samples C and D) and purified by using a Franz magnetic separator and heavy liquids (bromoform and alcohol). Mineral purifications were checked by optical and X-ray powder diffraction methods. Large-grained (15–20 μm), radiating clay minerals having second-order yellow polarization colors were observed in the clayey matrix of the prismatic horizon (E in Figure 1); these clay minerals were quite distinct from the weathering products of hornblende (smectite) and andesine (kaolinite) and were interpreted, on the basis of their crystallization sites, as the ultimate weathering products of the chlorites (Proust, 1983). Sufficient amounts of the pure clay minerals could not be separated from the bulk sample to yield reliable Mössbauer and infrared spectra; hence, only X-ray powder diffraction patterns and microprobe analyses were obtained from such materials.

[4] Vertically aligned, elongate, slicken sided blocks characterized by vertical fissure patterns.

X-ray powder diffraction

The X-ray powder diffraction (XRD) studies were carried out using a Philips P.W. 1730 diffractometer (40 kV, 40 mA) and Fe-filtered CoKα radiation. Samples were examined as random powders or parallel-oriented, K- or Mg-saturated specimens.

Mössbauer spectroscopy

Mössbauer spectra were obtained at 300 K with a constant acceleration spectrometer (Elscint, A.M.E. 30) employing a Promeda 1024 channel analyzer; a 25-mCi source of ^{57}Co in rhodium equipped with a solid-state NaI detector was used. The velocity calibration of the spectrometer was carried out with α-Fe at 300 K. One major difficulty with phyllosilicates is the preferred orientation of crystallites; texture effects tend to appear with the platelets in the plane of the absorber and may produce unequal intensity of the two lines of the quadrupole doublets (Nagly, 1978). Two methods are currently used to avoid such texture effects: the spectra can be recorded either with the normal of the absorber plane at 54.7° to the direction of the gamma-beam (Ericsson and Wäppling, 1976) or by using particles randomized by grinding with an inert powder (Coey, 1980). The second method was used in this work using colloidal graphite as the inert powder. For comparison purposes, 30 mg of material was used for each sample and about 2×10^6 counts were accumulated for each spectrum. The spectra, thus obtained from the 256 channels of the analyzer, were fitted by means of a least squares program to a sum of doublets having Lorentzian line shapes; the peaks of each doublet were constrained to have equal heights and widths. A χ^2 test was used as a goodness-of-fit parameter; for a fit to be acceptable, χ^2 had to be between 1 and 2.

Infrared spectroscopy

A mixture of 1 mg of pulverized chlorite and 300 mg of KBr was pressed under vacuum with an oil press to a disc of 13-mm diameter and 2-mm thickness. The pressure exerted on the samples was 10 kg/cm^2; the infrared (IR) spectra in the 4000–250-cm^{-1} region were recorded using a Beckman IR 4240 type infrared absorption spectrometer, and a 300-cm/min scanning speed.

Chemical analyses

The chemical analyses of the original and weathered chlorites were performed on diamond-polished thin sections using a Cameca MS 46 electron microprobe equipped with a Tracor energy-dispersive analyzer; data were refined using a correction program for atomic number (Z), absorption (A), and fluorescence (F) effects. A low-energy electron beam (1.5 nA, 15 kV) was used to minimize the loss of elements through volatilization during the counting time (120 s).

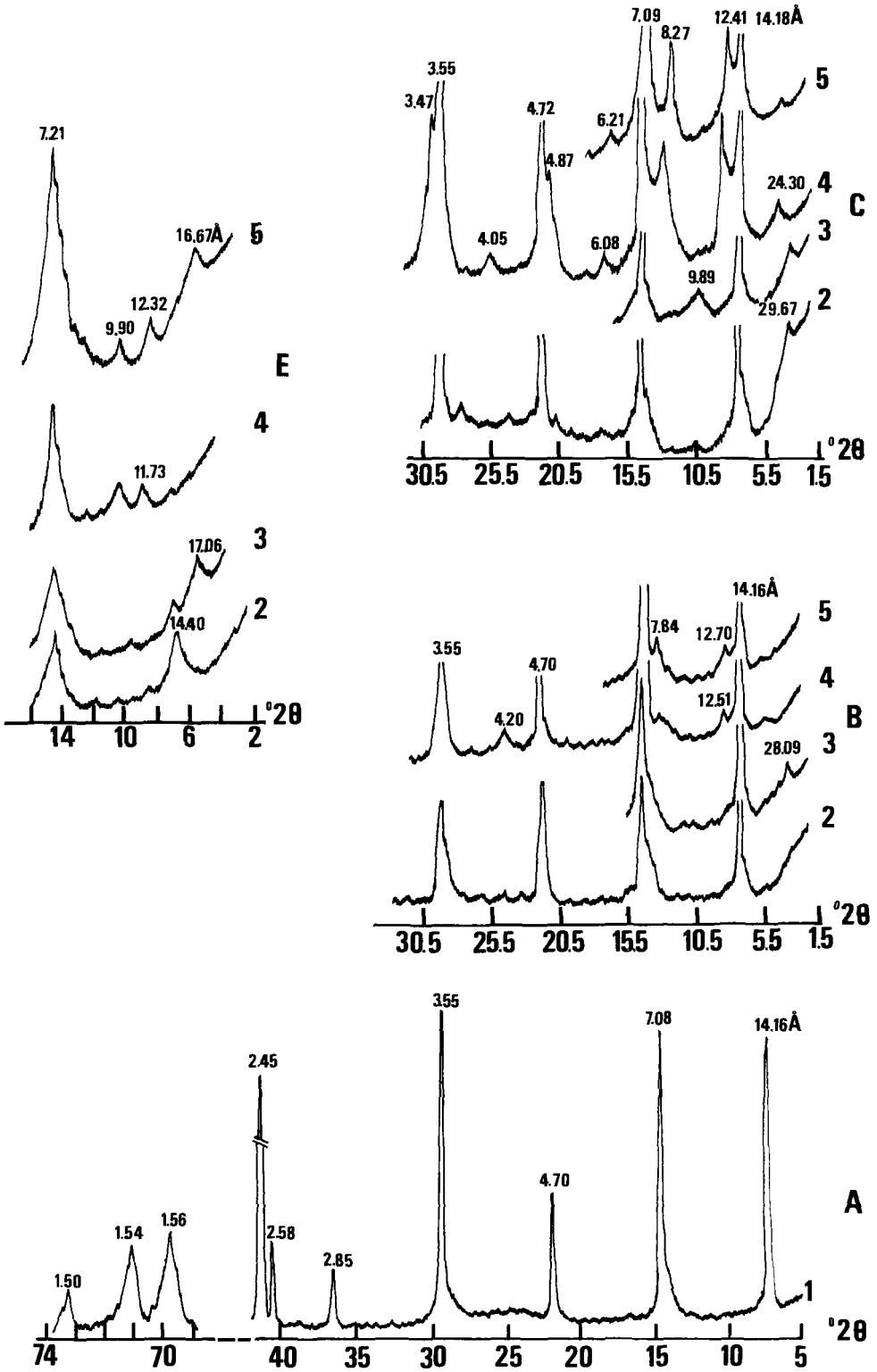

Figure 2. X-ray powder diffraction patterns of the original chlorite (sample A), interstratified chlorite/vermiculite (samples B and C) and vermiculite (sample E). 1 = random powder; 2 = Mg-saturated; 3 = Mg-saturated, glycolated; 4 = K-saturated; 5 = K-saturated, heated to 110°C, and glycolated (CoKα radiation).

https://doi.org/10.1346/CCMN.1986.0340511 Published online by Cambridge University Press

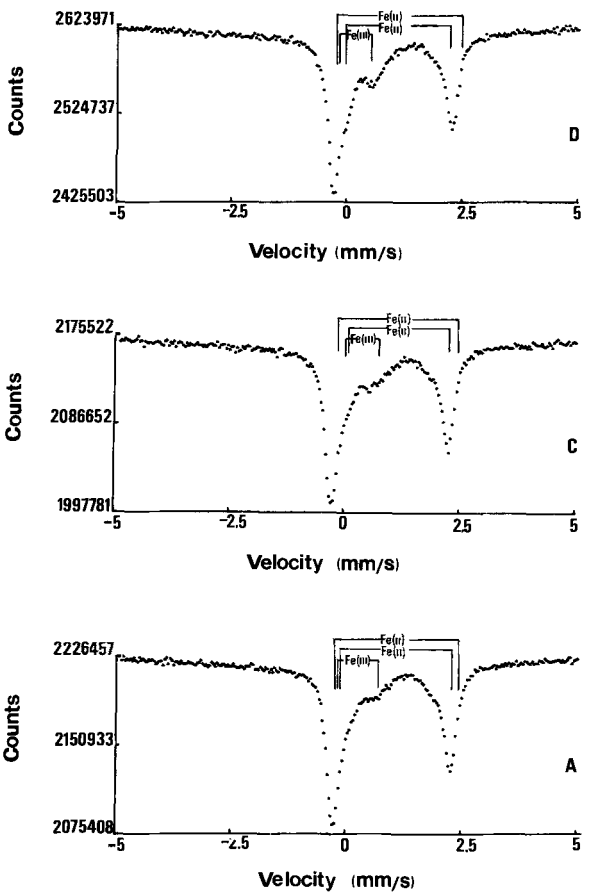

Figure 3. Mössbauer spectra of the original chlorite (sample A) and mixtures of chlorite and interstratified chlorite/vermiculite (samples C and D).

RESULTS AND DISCUSSION

X-ray crystallography

The XRD patterns of the original and weathered chlorites are illustrated in Figure 2. The original chlorite (sample A) gave a regular series of basal spacings at 14.16, 7.08, 4.70, 3.55, and 2.85 Å which did not change after ethylene glycol, potassium, or magnesium saturations. The 060 and 062 reflections at 1.54 and 1.50 Å revealed the trioctahedral character of the chlorite and the presence of a IIb structural unit (Shirozu, 1978; Bailey, 1980). The estimate of the total iron and of its distribution between the 2:1 mica layer and the hydroxide sheet of the original chlorite was made from the observed relative intensities of the 002, 003, 004, and 005 reflections (Brown and Brindley, 1980). Assuming a maximal error of 20% for the measurements (Brindley and Gillery, 1956), this procedure yielded a total iron content of 1.07 ± 0.21 atoms per 6.00 octahedral cations, with about 90% in the 2:1 mica layer and 10% in the hydroxide sheet.

The XRD patterns obtained from the saprock and the saprolite (samples B and C) suggest the presence of an ordered chlorite/vermiculite (C/V) interstratification together with relicts of the original chlorite. The ordered C/V is indicated by a rational series of 00*l* spacings with a periodicity of 29.67 Å in the Mg-saturated state, collapsing to 24.30 Å on K-saturation. These reflections did not shift if the K-saturated sample was heated to 110°C and solvated with ethylene glycol. It should be noted that the long-spacing ordering peak and the higher order reflections gained in resolution and intensity from the saprock to the saprolite; the best resolved pattern (sample C) approached the calculated XRD pattern of the fully ordered 1:1 C/V interstratification obtained by Reynolds (1980). These data suggest that the vermiculite component of the C/V structure increased with weathering. The lack of a reflection at 1.53 Å for samples B and C suggests that the vermiculite component is dioctahedral and has 060 reflection presumably superimposed on the 062 reflection of the chlorite relicts at 1.50 Å.

XRD patterns obtained from the prismatic horizon (sample E) indicate a mixture of kaolinite, smectite, and small amounts of vermiculite, as revealed by the 9.9-Å reflection of the K-saturated, heated-to-110°C, ethylene glycol-solvated sample. As mentioned above, microscopic examination and microprobe analyses of the primary mineral weathering microsites (not shown here) suggest that the kaolinite and smectite are products of weathering of andesine and hornblende, re-

Table 1. Mössbauer parameters of chlorite and interstratified chlorite/vermiculite.

	Fe^{2+}							Fe^{3+}			
Sample[1]	QS	IS	Γ	QS	IS	Γ	%	QS	IS	Γ	%
A	2.61	1.13	0.29	2.35	1.13	0.38	72	0.87	0.36	0.70	28
B	2.62	1.14	0.30	2.33	1.12	0.40	62	0.60	0.30	0.70	38
C	2.62	1.14	0.32	2.25	1.14	0.32	61	0.64	0.40	0.72	39
D	2.61	1.13	0.32	2.25	1.12	0.28	52	0.70	0.37	0.74	48

QS (quadrupole splitting), IS (isomer shift), and Γ (line width) are expressed in mm/s; uncertainty is parameters is 0.02 mm/s.

[1] Sample A = original chlorite from fresh rock; samples B, C, D = interstratified chlorite/vermiculite from the saprock (B) and saprolite (C and D).

https://doi.org/10.1346/CCMN.1986.0340511 Published online by Cambridge University Press

spectively. Microprobe analyses obtained from the coarse-grained, radiating clay minerals which originated from the weathering of chlorite gave chemical compositions of dioctahedral vermiculites.

The chlorite weathering process thus appears to be as follows: chlorite → ordered C/V (with increasing proportions of vermiculite layers) → vermiculite.

Mössbauer spectroscopy

The Mössbauer spectra of the original chlorite and a mixture of chlorite and C/V are shown in Figure 3; the spectra were computer fitted with one Fe^{3+} and two Fe^{2+} quadrupole doublets. The Mössbauer parameters obtained from the computer fit are listed in Table 1.

The Mössbauer data for the original chlorite (sample A) indicate that 72% of the total iron is present in the Fe^{2+} state. The quadrupole splitting (QS) and the isomer shift (IS) of the major Fe^{2+} doublet are similar to those obtained by Goodman and Bain (1979) for low-iron chlorites; moreover, they do not differ from those reported for biotites containing Fe^{2+} in octahedral coordination with OH in *cis* arrangement. The QS of the minor Fe^{2+} doublet has smaller value (2.35 mm/s) which can be assigned to Fe^{2+} in octahedral *trans* site (Häggström *et al.,* 1969; Sanz *et al.,* 1978). Furthermore, no Mössbauer absorption peak can be resolved within the QS range of 2.89–2.90 mm/s reported for Fe^{2+} in brucite (Ballet, 1979; Blaauw *et al.,* 1979; Coey, 1980; Heller-Kallai and Rozenson, 1981), indicating an absence of Fe^{2+} substitution in the hydroxide sheet, or, at the least, a very small amount of substitution, in good agreement with Fe distribution calculated from XRD spectra. The value of the IS for the Fe^{3+} doublet (0.36 mm/s) is similar to those reported for octahedral Fe^{3+} in chlorites and biotites (Goodman and Bain, 1979; Sanz *et al.,* 1978). Fe^{3+} substitution in the tetrahedral sheets thus can be excluded, because no Mössbauer absorption peak can be resolved within the IS range of 0.24–0.28 mm/s (Goodman and Bain, 1979; Heller-Kallai and Rozenson, 1981).

The Mössbauer spectra obtained from the mixture of chlorite and C/V (samples C and D) show no marked differences from the original chlorite. The calculated values of QS and IS for Fe^{2+} components are similar and can be assigned to octahedral Fe^{2+} sites with *cis* and *trans* OH groups. Thus, no Mössbauer evidence was found for Fe^{2+} substitutions in the hydroxide sheet. The IS of the Fe^{3+} component shows more scattering values in the range of 0.30–0.40 mm/s which are, however, characteristic of octahedral Fe^{3+} sites and no tetrahedral Fe^{3+} site.

The most prominent differences among the several samples were a general decrease of the Fe^{2+} line intensity and a slight increase of the Fe^{3+} line with degree of vermiculitization. These trends were confirmed by the progressive changes of the Fe^{2+} and Fe^{3+} contents,

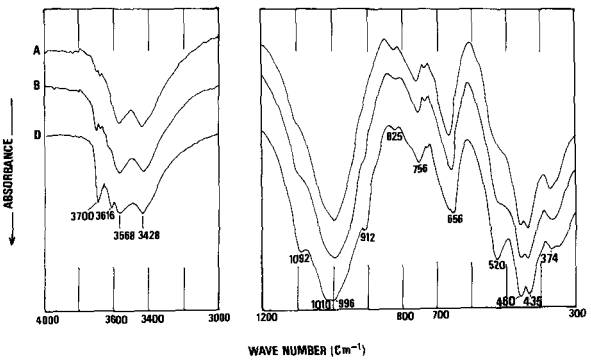

Figure 4. Infrared spectra of the original chlorite (A) and the mixtures of chlorite and interstratified chlorite/vermiculite (B and D).

as deduced from the relative areas of the absorption peaks (Table 1). Inasmuch as an Fe^{2+} decrease can be produced by $Fe^{2+} \rightarrow Fe^{3+}$ oxidation and/or Fe^{2+} leaching from the chlorite structure, the Mössbauer Fe^{2+}/Fe^{3+} ratio must be considered with respect to the total Fe content, as obtained by the electron microprobe analyses (*vide infra*). The QS values of the Fe^{3+} component, however, did not change with vermiculitization and are similar to that obtained for the original chlorite (0.60–0.87 mm/s). Typically, Fe^{3+} QS values of vermiculitized chlorites are much lower than those reported by Borggaard *et al.* (1982) for Fe^{3+} component formed by oxidation of structural Fe^{2+} (1.48–1.64 mm/s), suggesting that the oxidation of structural Fe^{2+} is limited in this vermiculitization process.

Infrared spectroscopy

The IR spectra obtained from the original chlorite and the mixture C/V and chlorite are shown in Figure 4. The assignments of the absorption bands follow those proposed by Serratosa and Vinas (1964), Hayashi and Oinuma (1965, 1967), and Farmer (1974).

The IR spectrum of the original chlorite shows three main absorption bands in the 4000–3000-cm^{-1} region which can be assigned to the OH-stretching vibrations in the 2:1 mica layer (3677 cm^{-1}) and the hydroxide sheet (3572 and 3432 cm^{-1}), respectively. The positions of the OH-bending (662 cm^{-1}), Al–O (760 and 822 cm^{-1}), and Si–O (998 and 458 cm^{-1}) vibrations are similar to those observed by Hayashi and Oinuma (1965), Post and Plummer (1972), and Farmer (1974) for low-iron chlorites.

Assignments of the weak, additional bands at 3700, 912, 520, and 435 cm^{-1} in the weathered chlorites are more difficult. The 3700-cm^{-1} absorption band was reported for C/V by Post and Janke (1974) and Dubinska (1982) and for expanding clay minerals containing synthetic Mg-hydroxy interlayers (Ahlrichs, 1968). These authors concluded that this absorption

https://doi.org/10.1346/CCMN.1986.0340511 Published online by Cambridge University Press

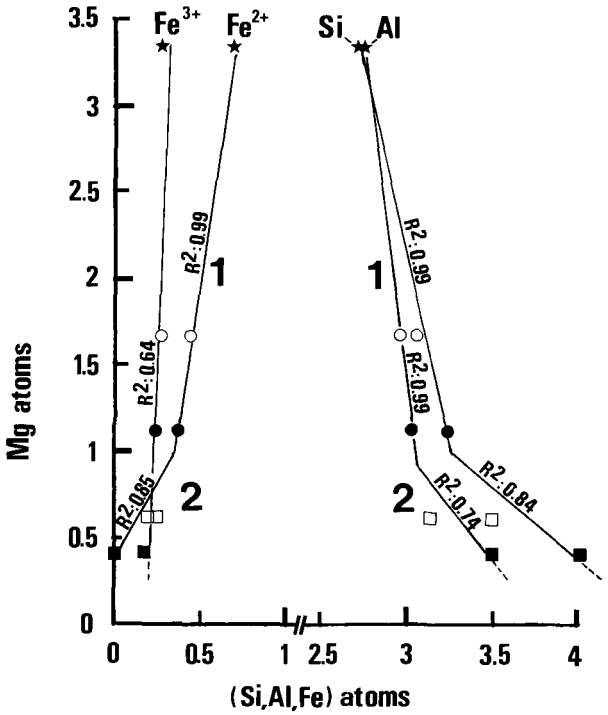

Figure 5. Plots of Mg vs. Si, Al, Fe contents of the original chlorite from sample A (★), interstratified chlorite/vermiculite from samples B (○), C (●), and D (□), and vermiculite from sample E (■).

band was produced by the vibration of magnesium hydroxide in partially degraded brucitic sheets. The development of a 3616-cm^{-1} band in the interstratified phase in sample D, together with 912- and 520-cm^{-1} bands, can be assigned to Al–AlOH-stretching (3616 cm^{-1}) and bending (912 cm^{-1}) vibrations (Lietzke and Mortland, 1973; Farmer, 1974), whereas the 520-cm^{-1} absorption band can be attributed to octahedral Al–O–Si vibrations (Hayashi and Oinuma, 1965). The absorption band at 435 cm^{-1} can be related to octahedral Fe–O–Si vibrations (Borggaard *et al.*, 1982). These five additional bands are apparently sensitive to the vermiculitization process, and their evolutions lead to the following:

1. The increasing intensity of the 3700-cm^{-1} band with increased vermiculitization indicates that increasing amounts of brucitic sheets are disrupted as a result of the release of Mg. Interlayer hydroxide sheets become discontinuous and are partly replaced by cation-water packets or sheets. The persistence of OH-stretching bands produced by undisturbed hydroxide sheets can be attributed to the chlorite component of the interstratified phase and/or to unweathered relicts of the original chlorite. IR spectroscopy cannot resolve this ambiguity.

2. The increasing intensity of the Al–AlOH and Al–O–Si absorption bands with vermiculitization points to an Al enrichment of the octahedral sheets in the interstratified phases. The development of a strong 1092-cm^{-1} absorption band in sample D indicates a decrease of the Al-for-Si tetrahedral substitutions with weathering (Farmer, 1974).

3. Borggaard *et al.* (1982) noticed a shift of the Si–O and Fe–O–Si vibrations to higher frequencies upon chlorite oxidation. These shifts were not observed in our IR spectra, indicating that Fe^{2+} oxidation was a minor process in this vermiculitization sequence.

Chemical microprobe analyses

Average microprobe analyses of the chlorite and of its weathering products are listed in Table 2. Fe^{2+} and Fe^{3+} contents were deduced from the Mössbauer data, except for vermiculite where all Fe was assumed to be in the Fe^{3+} state (no Mössbauer data were available for this mineral).

The average composition of the original chlorite falls in the magnesian chlorite field with a Fe/(Fe + Mg) atomic ratio <0.3 (Shirozu, 1978) and in the sheri-

Table 2. Average microprobe analyses of chlorite and of its vermiculitized weathering products.[1]

	A(8)	B(6)	C(8)	D(5)	E(8)
Si	2.71	3.05	3.24	3.50	3.15
Al(IV)	1.29	0.95	0.76	0.50	0.85
Al(VI)	1.45	2.01	2.27	2.64	1.90
Ti	0.01	0.01	0.01	0.01	0.01
Fe^{2+}	0.69	0.44	0.37	0.24	
Fe^{3+}	0.27	0.27	0.24	0.22	0.14
Mn	0.01	0.01	0.01	0.01	0.01
Mg	3.34	1.67	1.12	0.62	0.32
Ca	0.01	0.08	0.10	0.10	0.02
Na	0.01	0.01	0.04	0.01	0.01
K	0.01	0.04	0.07	0.06	0.02
Base	$O_{10}(OH)_8$	$O_{10}(OH)_8$	$O_{10}(OH)_8$	$O_{10}(OH)_8$	$O_{10}(OH)_2$

[1] Letters refer to sample locations in Figure 1; ( ) are number of analyses. A = original chlorite; B, C, D = interstratified chlorite/vermiculite; E = vermiculite calculated with total Fe expressed as Fe^{3+}.

https://doi.org/10.1346/CCMN.1986.0340511 Published online by Cambridge University Press

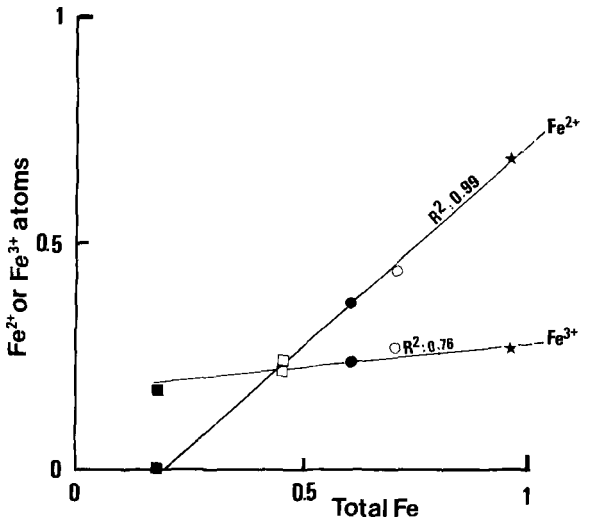

Figure 6. Plots of Fe^{2+} and Fe^{3+} contents vs. total Fe content of the original chlorite from sample A (★), interstratified chlorite/vermiculite from samples B (○), C (●), and D (□), and vermiculite from sample E (■).

danite field of Foster's classification (1962). The major element contents of the interstratified and vermiculitic phases are correlated in Figure 5. These data support the result of the above analyses, in that Mg and Fe^{2+} decrease, Si and Al increase, and Fe^{3+} remains constant with increasing vermiculitization. Two steps, however, can be inferred concerning the rates of release or enrichment. The first step is the weathering of chlorite into interstratified phases in the saprock and in the bottom part of the saprolite. Here, vermiculitization produces substantial Mg and Fe^{2+} releases, and a slight Si-Al enrichment, whereas Fe^{3+} remains nearly constant. The second step takes place at the top of the weathering profile where interstratified phases alter into dioctahedral vermiculites. Here, Mg and Fe^{2+} are released at equal rates, Si and Al are highly enriched, and Fe^{3+} is almost constant.

The chief structural changes induced by these chemical changes are a continuous decrease of the Al-for-Si tetrahedral substitutions together with a general increase of the Al-for-(Mg + Fe) octahedral substitutions with increased weathering. These changes agree well with the increasing dioctahedral character of the clay minerals, as observed in the XRD and IR spectra.

Iron oxidation state and release

The Fe^{2+} and Fe^{3+} contents, calculated on the same basis of 14 oxygens are correlated with total Fe in Figure 6. It should be noted first that vermiculitization induced a significant decrease in total Fe, mainly due to the release of Fe^{2+} from the chlorite structure. The Fe^{3+} contents remained nearly constant or, at least, did not increase. Second, the total Fe content of the vermiculite, initially assumed to be in Fe^{3+} state, correlates well with these results.

Table 3. Degree of interstratification and structural formulae of the interstratified chlorite/vermiculite.[1]

Degree of interstratification[2]	B		C		D	
	0.64 C	0.36 V	0.54 C	0.46V	0.35 C	0.65 V
Si	2.71	3.00	2.71	3.17	2.71	3.17
Al(IV)	1.29	1.00	1.29	0.83	1.29	0.83
Al(VI)	1.45	1.72	1.45	1.89	1.45	1.85
Ti	0.01	—	0.01	—	0.01	0.01
Fe^{2+}	0.64	—	0.61	—	0.60	—
Fe^{3+}	0.27	0.22	0.28	0.15	0.26	0.15
Mn	0.01	—	0.01	—	0.01	0.01
Mg	2.41	—	1.87	—	1.51	—
Ca	0.01	0.17	0.01	0.17	0.01	0.13
Na	0.01	—	0.01	0.07	0.01	0.01
K	0.01	0.08	0.01	0.11	0.01	0.07

[1] Letters refer to sample locations in Figure 1; samples B, C, D = interstratified chlorite/vermiculite from the saprock (B) and saprolite (C and D).

[2] Chlorite component (C) is calculated on $O_{10}(OH)_8$ base; vermiculite component (V) is calculated on $O_{10}(OH)_2$ base.

These data, together with the Mössbauer data, indicate that the behavior of Fe during this particular vermiculitization process can be explained by a complete release of the Fe^{2+} originally present in the 2:1 mica layer of the chlorite, whereas the initial Fe^{3+} content was almost entirely retained in the last-formed vermiculite structure. These results contradict those obtained on experimentally altered chlorites (Makumbi and Herbillon, 1972; Ross, 1975; Ross and Kodama, 1974, 1976; Senkayi *et al.*, 1981; Borggaard *et al.*, 1982) which suggested an initial oxidation of Fe^{2+} with subsequent loss of Fe^{3+} and Mg from the hydroxide sheet.

Degree of interstratification and magnesium release

Figure 6 indicates that the Fe^{2+} content differs markedly between two end-members, i.e., chlorite and vermiculite. Inasmuch as C/V is well fitted to that linear correlation, the Fe^{2+} contents can be used to estimate the degree of interstratification between the 100% chlorite and 100% vermiculite end-members. The results thus obtained (Table 3) are in good agreement with the IR data and indicate a gradual increase of the vermiculitic component with weathering. The degree of interstratification calculated for sample C, i.e., 55% chlorite layers, matches well the XRD data which approached the spectrum of a fully ordered 1:1 C/V interstratification (Reynolds, 1980).

Average structural formulae can be deduced from the interstratifications, assuming that the composition of the chloritic component was constant throughout the weathering profile and excluding its percentage from the interstratified phase composition (Table 3). It should

https://doi.org/10.1346/CCMN.1986.0340511 Published online by Cambridge University Press

be noted, however, that the Mg content of the interstratified phases, even when Mg is entirely in the chloritic component, is too low compared with original chlorite. This observation supports a high degree of Mg leaching during vermiculitization which leads to incomplete hydroxide sheets with atomic occupancy ranging from 1.66 to 0.83. The degradation of the hydroxide sheets was concluded from IR spectra by the increasing intensity of the 3700-cm^{-1} absorption band. Thus, the vermiculitization of chlorite appears to have been dominated by substantial leaching of Mg, preferentially from the hydroxide sheet of the original chlorite.

CONCLUSIONS

XRD, Mössbauer, and IR spectra and chemical microprobe analyses suggest that the vermiculitization of chlorite results in the formation of ordered interstratified chlorite/vermiculite that becomes increasingly enriched in the vermiculite component with increased weathering. This type of vermiculitization proceeds by means of a release of Fe^{2+} from the 2:1 mica layer of the chlorite. The initial Fe^{3+} content is almost the same as that of the last weathering product, i.e., pure dioctahedral vermiculite. Mg is largely and preferentially released from the hydroxide sheet of the chlorite, whereas Si and Al progressively increase with weathering.

This vermiculitization process, as far as Si, Al, and Mg are concerned, is in good agreement with currently accepted weathering mechanisms. It differs, however, slightly in the behavior of iron. In this occurrence, vermiculitization was not initiated by the oxidation of Fe^{2+}, but by the simultaneous leaching of Fe^{2+} and Mg. This process has been previously suggested by Bain (1977) for weathered chlorites in Scottish soils.

REFERENCES

Adams, W. A. (1976) Experimental evidence on the origin of vermiculite in soils on lower Paleozoic sediments: *Soil Sci. Soc. Amer. J.* **40,** 793–795.

Ahlrichs, J. L. (1968) Hydroxyl stretching frequencies of synthetic Ni-, Al-, and Mg-hydroxy interlayers in expanding clays: *Clays & Clay Minerals* **16,** 63–71.

Bailey, S. W. (1980) Structures of layer silicates: in *Crystal Structures of Clay Minerals and Their X-ray Identification,* G. W. Brindley and G. Brown, eds., Mineralogical Society, London, p. 91.

Bain, D. C. (1977) The weathering of chloritic minerals in some Scottish soils: *J. Soil Sci.* **28,** 144–164.

Ballet, O. (1979) Fe^{2+} dans les silicates lamellaires. Etude magnétique et Mössbauer: Thèse 3e cycle, Grenoble, France, 118 pp.

Blaauw, C., Stroink, G., Leiper, W., and Zentilli, M. (1979) Crystal-field properties of Fe in brucite $Mg(OH)_2$: *Phys. Stat. Sol.* **B92,** 639–643.

Borggaard, O. K., Lindgreen, H. B., and Mørup, S. (1982) Oxidation and reduction of structural iron in chlorite at 480°C: *Clays & Clay Mienrals* **30,** 353–363.

Brindley, G. W. and Gillery, F. H. (1956) X-ray identification of chlorite species: *Amer. Mineral.* **41,** 169–186.

Brown, G. and Brindley, G. W. (1980) X-ray diffraction procedures for clay minerals identification: in *Crystal Structures of Clay Minerals and Their X-ray Identification,* G. W. Brindley and G. Brown, eds., Mineralogical Society, London, 339–346.

Coey, J. M. D. (1980) Clay minerals and their transformations studied with nuclear techniques: the contribution of Mössbauer spectroscopy: *Atom. En. Rev.* **18,** 73–124.

Dubinska, E. (1982) Nickel-bearing minerals with chlorite-vermiculite intermediate structure from Szklary near Zabkowice Slaskie (Lower Silesia): *Arch. Miner.* **38,** 27–48.

Ericsson, T. and Wäppling, R. (1976) On texture effects in M1 3/2–1/2 Mössbauer spectra: *J. Phys.* **37,** C6-719–C6-723.

Farmer, V. C. (1974) The layer silicates: in *Infrared Spectra of Minerals,* V. C. Farmer, ed., Mineralogical Society, London, 331–363.

Foster, M. D. (1962) Interpretation of the composition and a classification of the chlorites: *U.S. Geol. Surv. Prof. Pap.* **414-A,** 33 pp.

Gilkes, R. J. and Little, I. P. (1972) Weathering of chlorite and some associations of trace elements in Permian phyllites in Southeast Queensland: *Geoderma* **7,** 233–247.

Goodman, B. A. and Bain, D. C. (1979) Mössbauer spectra of chlorites and their decomposition products: in *Proc. Int. Clay Conf., Oxford, 1978,* M. M. Mortland and V. C. Farmer, eds., Elsevier, Amsterdam, 65–74.

Häggström, L., Wäppling, R., and Annersten, H. (1969) Mössbauer study of iron-rich biotites: *Chem. Phys. Letters* **4,** 107–108.

Hayashi, H. and Oinuma, K. (1965) Relationship between infrared absorption spectra in the region 450–900 cm^{-1} and chemical composition of chlorite: *Amer. Mineral.* **50,** 476–483.

Hayashi, H. and Oinuma, K. (1967) Si–O absorption band near 1000 cm^{-1} and OH absorption bands of chlorite: *Amer. Mineral.* **52,** 1206–1210.

Heller-Kallai, L. and Rozenson, I. (1981) The use of Mössbauer spectroscopy of iron in clay mineralogy: *Phys. Chem. Miner.* **7,** 223–238.

Herbillon, A. J. and Makumbi, M. N. (1975) Weathering of chlorite in a soil derived from a chlorite schist under humid tropical conditions: *Geoderma* **13,** 89–104.

Johnson, L. J. (1964) Chlorite-vermiculite intergrade as a weathering product of chlorite in a soil: *Amer. Mineral.* **49,** 446–572.

Lietzke, D. A. and Mortland, M. M. (1973) The dynamic character of a chloritized vermiculite soil clay: *Soil Sci. Soc. Amer. Proc.* **37,** 651–656.

Makumbi, L. and Herbillon, A. J. (1972) Vermiculitisation experimentale d'une chlorite: *Bull. Gr. Fr. Argiles* **24,** 153–164.

Nagly, D. L. (1978) Deformation induced texture in Mössbauer absorbers: *Appl. Phys.* **17,** 269–274.

Post, J. L. and Janke, N. C. (1974) Properties of "swelling" chlorite in some Mesozoic formations of California: *Clays & Clay Minerals* **22,** 67–77.

Post, J. L. and Plummer, C. C. (1972) The chlorite series of Flagstaff Hill area, California: a preliminary investigation: *Clays & Clay Minerals* **20,** 271–283.

Proust, D. (1983) Mécanismes de l'altération supergène des roches basiques. Etude des arènes d'orthoamphibolite du Limousin et de glaucophanite de l'île de Groix (Morbihan): Thèse Doct. Etat, Poitiers, 197 pp.

Rabenhorst, M. C., Fanning, D. S., and Foss, J. E. (1982) Regularly interstratified chlorite/vermiculite in soils over

meta-igneous mafic rocks in Maryland: *Clays & Clay Minerals* **30,** 156–158.

Reynolds, R. C. (1980) Interstratified clay minerals: in *Crystal Structures of Clay Minerals and Their X-ray Identification,* G. W. Brindley and G. Brown, eds., Mineralogical Society, London, p. 287.

Ross, G. J. (1975) Experimental alteration of chlorites into vermiculites by chemical oxidation: *Nature* **255,** 133–134.

Ross, G. J. and Kodama, H. (1974) Experimental transformation of a chlorite into a vermiculite: *Clays & Clay Minerals* **22,** 205–211.

Ross, G. J. and Kodama, H. (1976) Experimental alteration of a chlorite into a regularly interstratified chlorite/vermiculite by chemical oxidation: *Clays & Clay Minerals* **24,** 184–190.

Ross, G. J., Wang, C., Ozkan, A. I., and Rees, H. W. (1982) Weathering of chlorite and mica in a New Brunswick podzol developed on till derived from chlorite-mica schist: *Geoderma* **27,** 255–267.

Sanz, J., Meyers, J., Vielvoye, L., and Stone, W. E. E. (1978) The location and content of iron in natural biotites and phlogopites: a comparison of several methods: *Clay Miner.* **13,** 45–52.

Senkayi, A. L., Dixon, J. B., and Hossner, L. R. (1981) Transformation of chlorite to smectite through regularly interstratified intermediates: *Soil Sci. Soc. Amer. J.* **45,** 650–656.

Serratosa, J. M. and Vinas, J. M. (1964) Infra-red investigation of the OH bands in chlorites: *Nature* **202,** p. 199.

Shirozu, H. (1978) Chlorite minerals: in *Clays and Clay Minerals of Japan,* T. Sudo and S. Shimoda, eds., Elsevier, Amsterdam, 243–264.

(Received 9 September 1985; accepted 26 April 1986; Ms. 1518)